Asian Journal of Chemistry; Vol. 27, No. 9 (2015), 3308-3314

ASIAN JOURNAL OF CHEMISTRY

http://dx.doi.org/10.14233/ajchem.2015.18610

Adsorption of Ag(I), Cr(VI) and Pb(II) from Aqueous Media onto Different Adsorbent Types

M. ADNAN YOUNIS[1], RAZIYA NADEEM[1,*], ASMA REHMAN[2], MUNAWAR IQBAL[3,4,*], M. RIZWAN YOUNIS[2] and QAISAR MANZOOR[1]

[1]Department of Chemistry, University of Agriculture, Faisalabad-38040, Pakistan
[2]National Institute for Biotechnology and Genetic Engineering, Faisalabad, Pakistan
[3]National Centre of Excellence in Physical Chemistry, University of Peshawar, Peshawar-25120, Pakistan
[4]Department of Chemistry, COMSATS Institute of Information Technology, Abbottabad 22060, Pakistan

*Corresponding authors: E-mail: raziyaanalyst@yahoo.com; bosalvee@yahoo.com

Received: 18 August 2014; *Accepted*: 28 October 2014; *Published online*: 26 May 2015; AJC-17246

Adsorption of Ag(I), Cr(VI) and Pb(II) onto iron magnetic nanoparticles, chitosan–magnetite nanocomposite, calcium algenate beads and calcium alginate fungal beads (CAFB) were studied as a function of initial concentration, pH and contact time. The equilibrium adsorption data was analyzed using pseudo-first order and pseudo-second order kinetic models and Langmuir and Freundlich isotherms. The chitosan–magnetite nanocomposite and calcium alginate fungal beads showed significantly higher metal ion adsorption efficiency as compared to iron magnetic nanoparticles and calcium algenate beads. The sorption capacities of adsorbents varied with initial solution pH, metal ions concentration and contact time. Freundlich model fitted well to the data and the pseudo-second order described best the sorption kinetics.

Keywords: Heavy metals adsorption, Nanoparticles, Chitosan, Kinetics, Isotherms.

INTRODUCTION

To date, the contamination of heavy metal ions with water bodies and industrial wastewater is an important environmental issue. Heavy metal ions released into the environment from various sources and their removal is a real challenge due to their trace quantities, formation of complexes with natural organic matter and toxic even at very low concentrations[1]. Heavy metal ions are persistent pollutant and are not biodegradable and cannot be metabolized or decomposed naturally. Heavy metals can easily enter into the food chain through a number of pathways and cause progressive toxic effects with gradual accumulation in living organisms[2]. Many toxic metal along with other pollutants are often detected in industrial wastewater which originates from metal plating, mining activities, smelting, battery manufacture, printing, paint and pigment industries *etc.*[3-6].

Chromium is commonly used in industrial application, such as in tanning processes, electroplating, pigmentation, catalyst for corrosion inhibitors and wood preservatives. While hexavalent and trivalent species of chromium are prevalent in industrial wastes, the hexavalent form is considered hazardous to health due to its mutagenic and carcinogenic properties. The US EPA has set the maximum Cr(VI) level domestic water supplies[7] at 0.05 mg L^{-1}. The excellent malleability, ductility, electrical and thermal conductivity, photosensitivity and antimicrobial properties of silver make it a very useful raw material in various industries. Significant amounts of silver is, therefore lost in the effluents discharged from such industries and the toxicity of silver to living organisms warrants immediate removal of this metal from wastewaters[8]. Lead(II) also poses a significant threat to the environment and health due to its toxicity, incremental accumulation in the food chain due to its persistent nature in the ecosystem. Lead(II) is introduced into natural water bodies from paper and pulp, mining, electroplating, lead smelting and metallurgical finishing, dyeing, storage-battery and automotive industries[9]. Due to toxic nature and environmental impacts of heavy metals, environmental scientists are focusing studies for the removal heavy metal ions from wastes[3,10,11] which is good step to save the environment as a results of human activities in all field of life[12-16].

The techniques that have been widely used to remove toxic heavy metals from industrial effluents are ion exchange, chemical precipitation, complexation, elecrodeposition, liquid–liquid extraction, reverse osmosis, oxidation–reduction process, evaporation, membrane separation and adsorption. But these methods are expensive and ineffective especially when the heavy metal ions are present in the wastewater at low concentrations. Adsorption is one of the most economical, effective and widely used methods for the removal of heavy metals from aqueous environment[3,9,17,18].

Various researchers have been focused on the utilization of modified chitosan[17] and other immobilized biomass for the adsorption of heavy metals[19]. These techniques increases the

accessibility of binding sites and improves the mechanical stability[20]. Several studies of metal ion adsorption by modified chitosan have been carried out in recent years, such as composite chitosan biosorbent[17], chitosan biopolymer[21], cross-linked magnetic chitosan-2-aminopyridine glyoxal[22], chitosan–coated sand[20], chitosan immobilized on bentonite[23], chitosan coated PVC beads[24], H_2SO_4 modified chitosan[25], chitosan crosslinked with epichlorohydrin-triphosphate[26], cross-linked magnetic chitosan-phenylthiourea resin[27], hydroxyapatite/chitosan composite[28], chitosan-tripolyphosphate beads[29] and glutaraldehyde cross linked chitosan beads[30]. The immobilized calcium alginate and fungal biomass has been also used commonly for the removal of heavy metals form aqueous solutions for the remediation of environment[31-35].

Present study was designed to appraise the efficiency of the iron magnetic nanoparticles (IMNP), chitosan–magnetite nanocomposites (CMN), calcium algenate beads (CAB) and calcium alginate fungal beads (CAFB) for chromium, lead and silver ions removal from aqueous solutions. Experimental parameters affecting the adsorption process such as pH, initial metal ions concentration and contact time were studied. The experimental equilibrium adsorption data was analyzed by kinetic and isotherm models.

EXPERIMENTAL

All chemicals and reagents used were of analytical reagent grade; $FeCl_2$, $FeCl_3$, carbamide and polyacrylic acid, HCl, CH_3COOH, NaOH, Na_2HPO_4, KH_2PO_4, $K_2Cr_2O_7$, $CaCl_2$ and Na-alginate were purchased from E. Merck Company (Darmstadt, Germany). Pb(II), Cr(II) and Ag(II) standards were purchased from Fluka. Stock solution of heavy metals ions were prepared from salts of Pb(II), Cr(VI) and Ag(I) in bi-distilled water.

Adsorbent preparation and adsorption experiments: The iron magnetic nanoparticles, chitosan–magnetite nanocomposites, alginate and fungal beads were prepared following reported methods[36-39]. The demonstration of magnetic iron oxide nanopartice is shown in Fig. 1. To study the adsorption as a function of pH, 1-6 pH for Ag(I) and Pb(II), whereas 1-7 pH for Cr(VI), contact time (0-1400 min) and initial metal ions concentration (25-150 mg/L) were considered. The other variables such as adsorbent dose (100 m/L), temperature (room temperature) and shaking speed (50 rpm) during adsorption were kept constant. The Pb(II), Ag(I) and Cr(VI) concentration were determined using A Analyst 30, Perkin Elmer equipped with single element hollow cathode lamp and acetylene air source. The amount of metals adsorbed onto adsorbent was calculated by the simple concentration difference method. The adsorption capacities of adsorbents were estimated using the amount of ions retained on unit mass of adsorbent (eqn. 1)[9].

$$q = \frac{(C_0 - C) \times (V / 1000)}{m} \quad (1)$$

where C_0 is the initial concentration of chromium (mg/L), C is the equilibrium concentration (mg/L), V is the volume of solution (mL) and m is the adsorbent mass (g).

Statistical analysis: The data represents the mean of three independent experiments. The regression coefficient (R^2) values of the Langmuir isotherm, Freundlich isotherm, pseudo-first-order and pseudo-second-order models were determined using statistical functions of Microsoft Excel (version Office XP, Microsoft Corporation, USA)[9].

Fig. 1. Demonstration of magnetic iron oxide nanoparticles: (a) magnetic particles dispersed in water (b) their retention towards magnet

RESULTS AND DISCUSSION

Influence of initial metal concentration: Initial metal concentration is considered very important to overcome mass transfer resistance of the metal between the aqueous solution and solid phase. The influence of initial metal ion concentrations on uptake capacities of the adsorbents were studied at pH 5 for Pb(II) and Ag(I) and at pH 2 for Cr(VI). The concentration range of metals ions were studied from 25 to 150 mg/L and adsorption responses can be seen in Fig. 2. In case of Pb(II), the sorption capacities (q mg g^{-1}) increased from 24.38 to 78.66 mg g^{-1} for iron magnetic nanoparticles, 24.45-80.66 mg g^{-1} for chitosan–magnetite nanocomposite, 24.41-91.9 mg g^{-1} for calcium algenate beads and 24.43-118.58 mg g^{-1} for calcium alginate fungal beads when initial metal ion concentration increased from 25 to 100 mg/L for iron magnetic nanoparticles and chitosan–magnetite nanocomposite and 25-150 mg/L for calcium algenate beads and calcium alginate fungal beads. However, by increasing the initial metal ion concentration, the percentage removal decreased. The percentage removal decreased from 99.5 to 91.89 %, 99.80 to 94.23 %, 99.63 to 61.43 % and 99.71 to 79.26 % for iron magnetic nanoparticles, chitosan–magnetite nanocomposite, calcium algenate beads and calcium alginate fungal beads, respectively. The Ag(I) sorption capacities increased from 20.77 to 74.96 mg g^{-1}, 24.85 to 94.79 mg g^{-1}, 20 to 96.8 mg g^{-1} and 24.05 to 129.99 mg g^{-1} for iron magnetic nanoparticles, chitosan–magnetite nanocomposite, calcium algenate beads and calcium alginate fungal beads, respectively by increasing the initial concentration from 25 to 150 mg/L. The Cr(IV) sorption capacities (q mg g^{-1}) increased from 20 to 71.46 mg g^{-1}, 24.79 to 94.36 mg g^{-1}, 20.15 to 96.8 mg g^{-1} and 23.76 to 126.4 mg g^{-1} for iron magnetic nanoparticles, chitosan–magnetite nanocomposite, calcium algenate beads and calcium alginate fungal beads, respectively. In case of Ag(I) and Cr(VI) the percentage removal again decreased by increasing the metal initial concentration. Among all the adsorbent investigated, calcium alginate fungal beads showed maximum metal adsorption capacity and order for the removal of metallic ions [Ag(I), Pb(II) and Cr(VI)] was found as; calcium alginate fungal beads > calcium algenate beads > chitosan–magnetite nanocomposite > iron magnetic

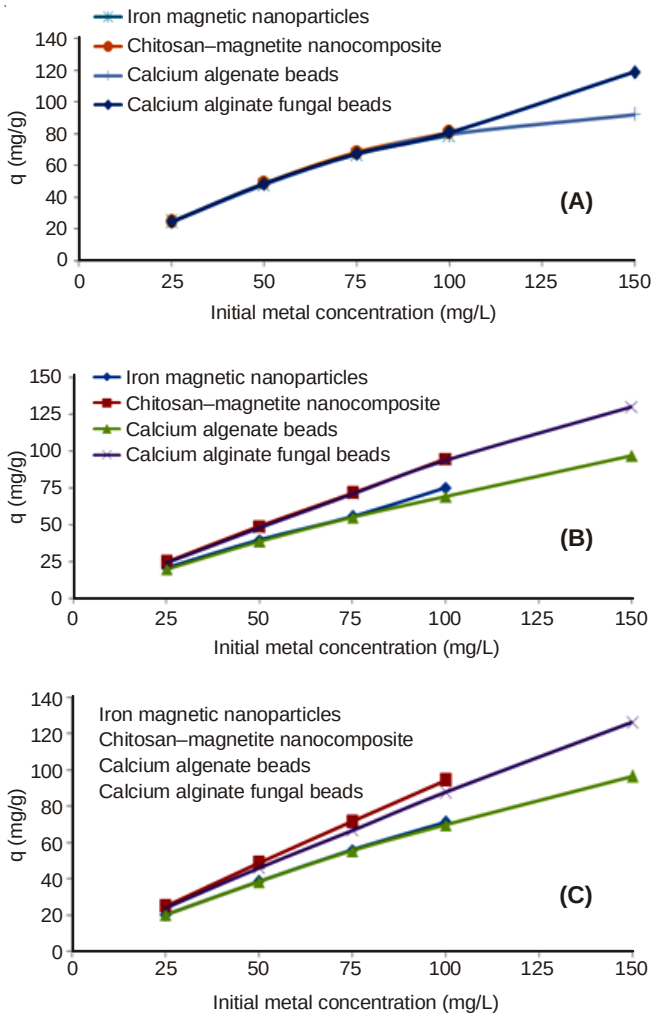

Fig. 2. Effect of metal ion concentrations on adsorption of Pb(II) (A), Ag(I) (B) and Cr(VI) (C): iron magnetic nanoparticles-iron magnetic nanoparticles, chitosan–magnetite nanocomposite-chitosan–magnetite nanocomposites, chitosan–magnetite nanocomposite-calcium algenate beads and calcium alginate fungal beads – calcium alginate fungal beads

nanoparticles. Results showed that the removal efficiency (q mg g^{-1}) increased by increasing the metal ions initial concentration. This might be due to the available of number of moles of metals to the surface area and functional adsorption became dependent on initial concentration. The initial concentration provides an important driving force to overcome all mass transfer resistance of metal ion between the aqueous and solid phases[9]. This may be explained by the fact that at very low concentration of metal ions, the ratio of sorption surface area to the total metal ions was high and metals ions were unable to diffuse. However, at higher concentrations, the diffusion to the adsorbent surface by inter particle diffusion may occur[40]. The decrease in percentage adsorption may be attributing to lack of sufficient surface area to mount up much more metal ions accessible in solution[2]. The results obtained from this investigation were found to be similar with many other reported work for Pb(II) and Ag(I) onto calcium algenate biomass beads[41], immobilized iron magnetic nanoparticles for Cr(VI)[42] calcium algenate biomass beads[43] and onto immobilized iron magnetic nanoparticles[44].

Influence of contact time: To evaluate the effect of contact time, the adsorption experiment was carried out with different time intervals ranging from 10 to 1440 min, while keeping the other parameter constant. The results showed that percentage removal of metallic ions increased by increasing the contact time initially, then become almost stable, denoting attainment of equilibrium. The sharp increase was observed in first 2 h and attained equilibrium at 4 h. So, equilibrium reached in a contact time of 4 h, at this point the amount of ions being adsorbed onto adsorbent was in a state of dynamic equilibrium with the amount desorbed from the adsorbent. This state of equilibrium was termed as the equilibrium time which reflected the maximum ions sorption capacity. In first 2 h, the fast adsorption was probably due to the fact that, initially the sites on adsorbent were vacant and the solute concentration was high and beyond this period no significant increase in metal ions uptake was observed which may be due to the saturation of active sites on the surface of sorbents. It is reported that more functional groups may participate in adsorption of the metal ions until equilibrium reached as a function of contact time[2]. In case of Ag(I), at equilibrium condition, the order of sorption capacity was as; chitosan–magnetite nanocomposite (93.97 mg g^{-1}) > calcium alginate fungal beads (93.48 mg g^{-1}) > calcium algenate beads (83.41 mg g^{-1}) > iron magnetic nanoparticles (73.3 mg g^{-1}) (Fig. 3a). In case of Cr(VI), the adsorption order was observed as; chitosan–magnetite nanocomposite (95.21 mg g^{-1}) > calcium alginate fungal beads (91.03 mg g^{-1}) > iron magnetic nanoparticles (75.43 mg g^{-1}) > calcium algenate beads (68.75 mg g^{-1}) at the equilibrium time (Fig. 3b). The trend of Pb(II) adsorption was found similar to Ag(I) (Fig. 3c). The data showed that the adsorption took place in two steps, a rapid surface adsorption within first 2 h and slow intercellular adsorption later on. It is well known that rapid initial sorption is due to extracellular binding and slow sorption results from intracellular binding[2,3]. This two stage sorption mechanism *i.e.* first rapid and quantitatively predominant and the second slower and quantitatively insignificant, has also been reported in literature based on adsorption of heavy metal ion adsorption onto plant biomass[9].

Influence of pH on adsorption: The pH of aqueous solution is a critical parameter in adsorption as it strongly affects metal sorption through surface charge and ionization process. It affects the solution chemistry and functional groups activity on the biomass surface and interaction of metallic ions as well. To understand the adsorption of Ag(I), Cr(VI) and Pb(II) as a function of pH, a range of pH was studied and results are shown in Fig. 4. The effect of pH on the adsorption capacity of sorbents, a pH range of 1-6 for Ag(I) and 1-7 for Cr(VI) and Pb(II) were studied. In case of Ag(I) the sorption capacity (q mg g^{-1}) increased from 16.96 to 64.41 mg g^{-1}, 21.1 to 88.74 mg g^{-1}, 25.8 to 82.79 mg g^{-1} and 30.57 to 93.14 mg g^{-1} for iron magnetic nanoparticles, chitosan–magnetite nanocomposite, calcium algenate beads and calcium alginate fungal beads, respectively when pH increased from 1 to 5. For Cr(VI), the maximum adsorption was observed at pH 2. The adsorption capacities of iron magnetic nanoparticles, chitosan–magnetite nanocomposite, calcium algenate beads and calcium alginate fungal beads increased from 40.35 to 73.69 mg g^{-1}, 53.69 to

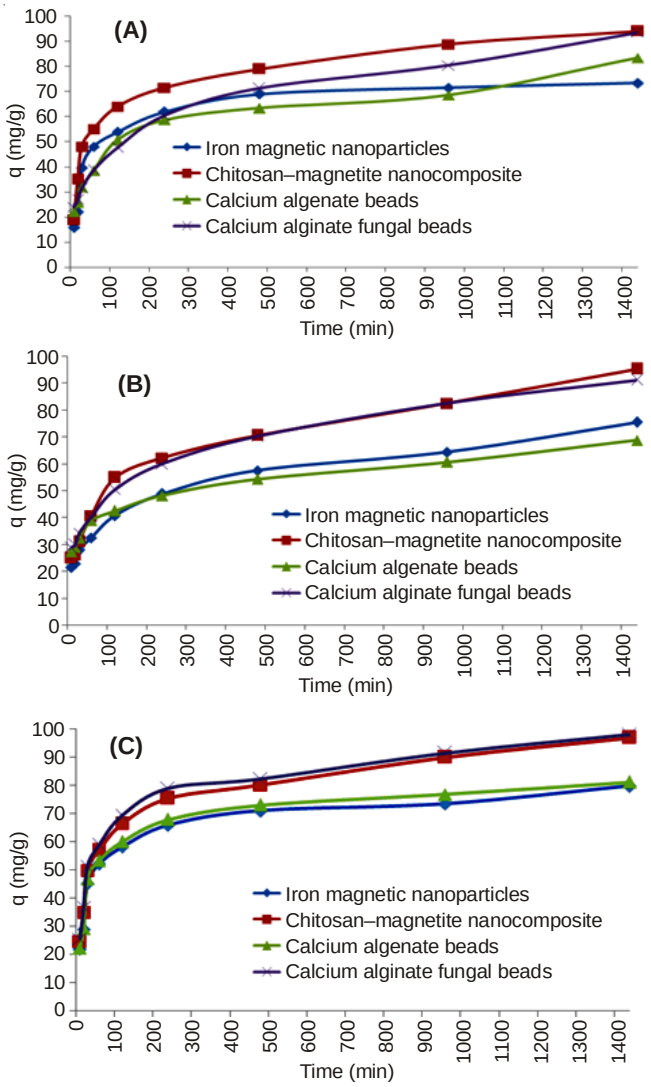

Fig. 3. Effect of contact time on (A) Ag(I), (B) Cr(VI) and (C) Pb(II) adsorption (explanations as given in Fig. 2)

93.48 mg g^{-1}, 40.77 to 67.21 mg g^{-1} and 58.81 to 88.75 mg g^{-1} as pH increased from 1-2 and further increase in pH decreased the adsorption capacity from 73.69 to 28.75 mg g^{-1}, 93.48 to 38.77 mg g^{-1}, 67.21 to 30.86 mg g^{-1} and 88.75 to 35.48 mg g^{-1} in case of iron magnetic nanoparticles, chitosan–magnetite nanocomposite, calcium algenate beads and calcium alginate fungal beads, respectively. Similar to Ag(I) adsorption, the Pb(II) adsorption was also recorded to be maximum at pH 5 for all type of adsorbents (Fig. 4c). The results clearly showed that pH play a significant role in the adsorption of Ag(I), Cr(VI) and Pb(II) onto all types of adsorbents under investigation. The lower adsorption at low pH may be due to the fact that overall surface charges become positive, which inhibits the approach of positively charged metal cations. It is likely that protons compete with metal ions for the ligands and thereby decrease the interaction of metal ion with the adsorbent. As the pH increased there is a net negative charge on the cell wall components that will promote reaction with metal cations. Moreover, as the pH increased the ligands (carboxyl, sulfhydryl, phosphate, *etc*.) expose which increases the negative charge density on the surface, resulting in greater attraction between metallic ions and ligands[45].

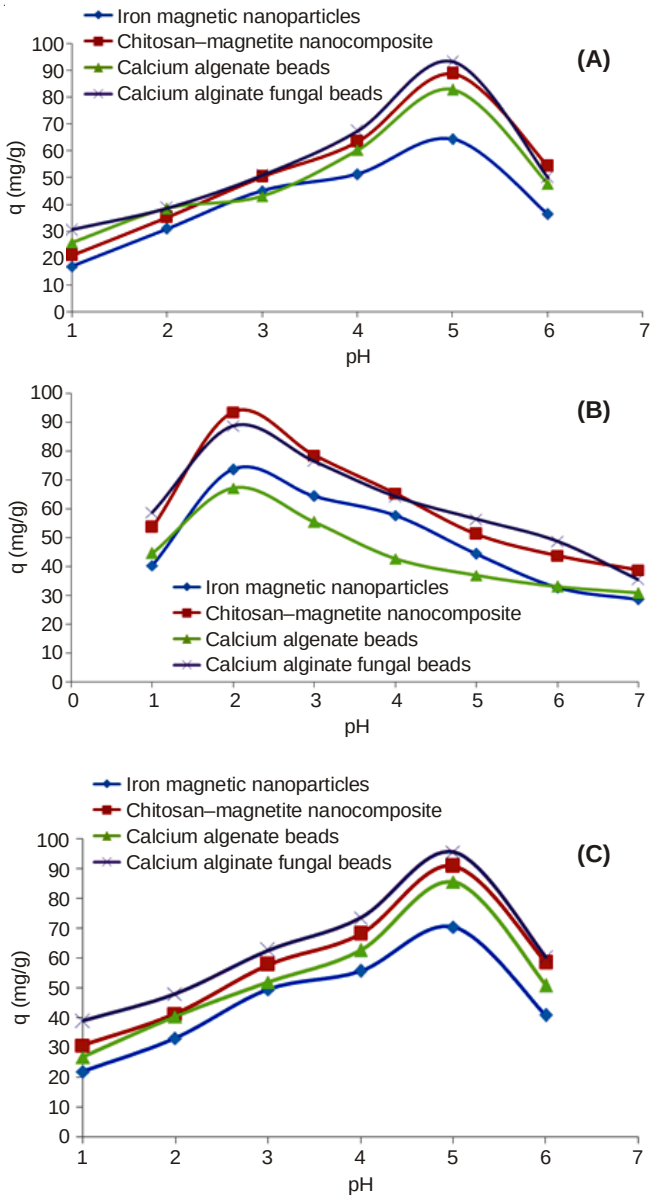

Fig. 4. Effect of pH on (A) Ag(I), (B) Cr(VI) and (C) Pb(II) adsorption (explanations as given in Fig. 2)

Adsorption isotherms: The adsorption isotherms are characterized by definite parameters, whose values express the surface properties and affinity of sorbent for heavy metal ions adsorption[2]. Two isotherm models were selected to fit the experimental data, namely Langmuir and Freundlich isotherm models. The mathematical expressions of isotherm models are represented in eqns. 2 and 3, respectively.

$$\frac{C_e}{q_e} = \frac{1}{q_{max} K_L} + \frac{C_e}{q_{max}} \quad (2)$$

$$\log q_e = \frac{1}{n(\log C_e)} + \log k \quad (3)$$

where q_e is the metal ion adsorbed (mg/g), C_e the equilibrium concentration of metal ion solution and K_L and k and 1/n are the Langmuir and Freundlich equations constants, respectively.

The Langmuir isotherm assumes that solid surface has a finite number of identical sites which are energetically uniform. According to this model, all adsorbed species interact only

with a site instead of each other and the adsorption is limited to monolayer. It is then assumed that once a metal ion occupies a site, no further sorption can take place. Freundlich isotherm equation assumes that a multilayer sorption with a heterogeneous energetic distribution of active sites, accompanied by interaction between adsorbed molecules and is an empirical relationship which describes the adsorption of solutes from a liquid to a solid surface[36]. The linear plot of the Freundlich isotherm model for sorption is presented in Fig. 5. For Freundlich isotherm model, the R^2 values with respect to the sorption of Ag(I) was noted to be 0.973, 0.884, 0.968 and 0.960 and for Cr(VI) 0.921, 0.881, 0.971 and 0.958 for iron magnetic nanoparticles, chitosan–magnetite nanocomposite, calcium algenate beads and calcium alginate fungal beads, respectively. For Langmuir isotherm model, the R^2 values with respect to the sorption of Ag(I) was noted to be 0.785, 0.951, 0.877 and 0.830 and 0.832, 0.787, 0.874 and 0.903 in case Cr(VI) for iron magnetic nanoparticles, chitosan–magnetite nanocomposite, calcium algenate beads and calcium alginate fungal beads, respectively.

Similar trend was observed for Pb(II) both for Freundlich and Langmuir isotherms. The values of R^2 were found to be smaller for Langmuir model *versus* Freundlich model for all types of sorbents for the adsorption of Ag(I), Cr(VI) and Pb(II). The R^2 and q_{max} values for Ag(I), Cr(VI) and Pb(II) suggested that the Freundlich isotherm model described the sorption well as compared to Langmuir model.

Kinetic modelling: In order to examine the mechanism of adsorption and potential rate controlling step, such as mass transport and chemical reaction processes, kinetic models have been used to test the experimental data. A kinetic study with dissimilar time intervals with fixed metal and adsorbent concentration was performed. Kinetics of absorption has been extensively examined by first order expression given by Lagergren's pseudo-first-order and pseudo second order approach, eqns. 4 and 5.

$$\log (q_e - q_t) = \log q_e - \left\{ k_{1,ads} \frac{t}{2.303} \right\} \quad (4)$$

$$\frac{t}{q_t} = \frac{1}{k_{2,ads} q_e^2} + \frac{t}{q_e} \quad (5)$$

where q_e is the mass of metal adsorbed at equilibrium (mg g^{-1}), q_t is the mass of metal at time t (min), $k_{1,ads}$ is the first order reaction rate constant of adsorption (min^{-1}), $k_{2,ads}$ is the pseudo-second order rate constant of adsorption (mg g^{-1} min^{-1}).

A comparison between pseudo first order and pseudo second order kinetic model plots are shown in Fig. 6. The results indicated that 71.25, 83.71, 75.46 and 88.48 mg g^{-1} of Ag(I) and 59.46, 89.67, 62.63 and 84.56 mg g^{-1} of Cr(VI) were adsorbed on to iron magnetic nanoparticles, chitosan–magnetite nanocomposite, calcium algenate beads and calcium alginate fungal beads, respectively. The estimated q_e values for pseudo-second order kinetic model was found to be in accordance with the q_{exp} (exp) [73.3, 93.97, 83.41 and 93.48 mg g^{-1} for Ag(I)] and [75.43, 95.21, 68.75 and 91.03 mg g^{-1} for Cr(VI)] sorption onto iron magnetic nanoparticles, chitosan–magnetite nanocomposite, calcium algenate beads and calcium alginate fungal beads, respectively. The kinetic behaviour of Pb(II) was found similar to Ag(I). Data confirms that pseudo-first order kinetic model was not best to describe the sorption kinetics of Ag(I), Cr(VI) and Pb(II) for the adsorption onto iron magnetic nanoparticles, chitosan–magnetite nanocomposite, calcium algenate beads and calcium alginate fungal

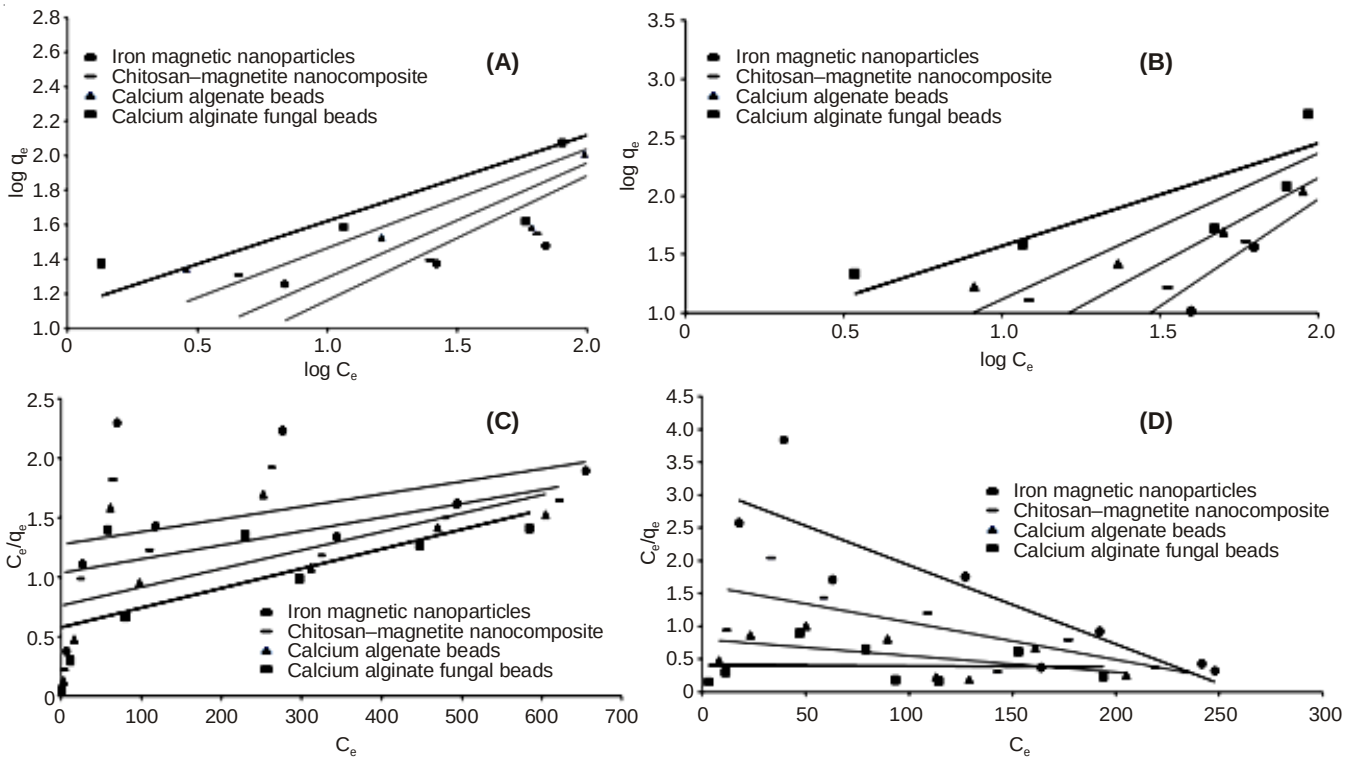

Fig. 5. Comparison of isotherm models: (A) and (B) Freundlich model for Ag(I) and Cr(VI), (C) and (D) Langmuir models for Ag(I) and Cr(VI), respectively (explanations as given in Fig. 2)

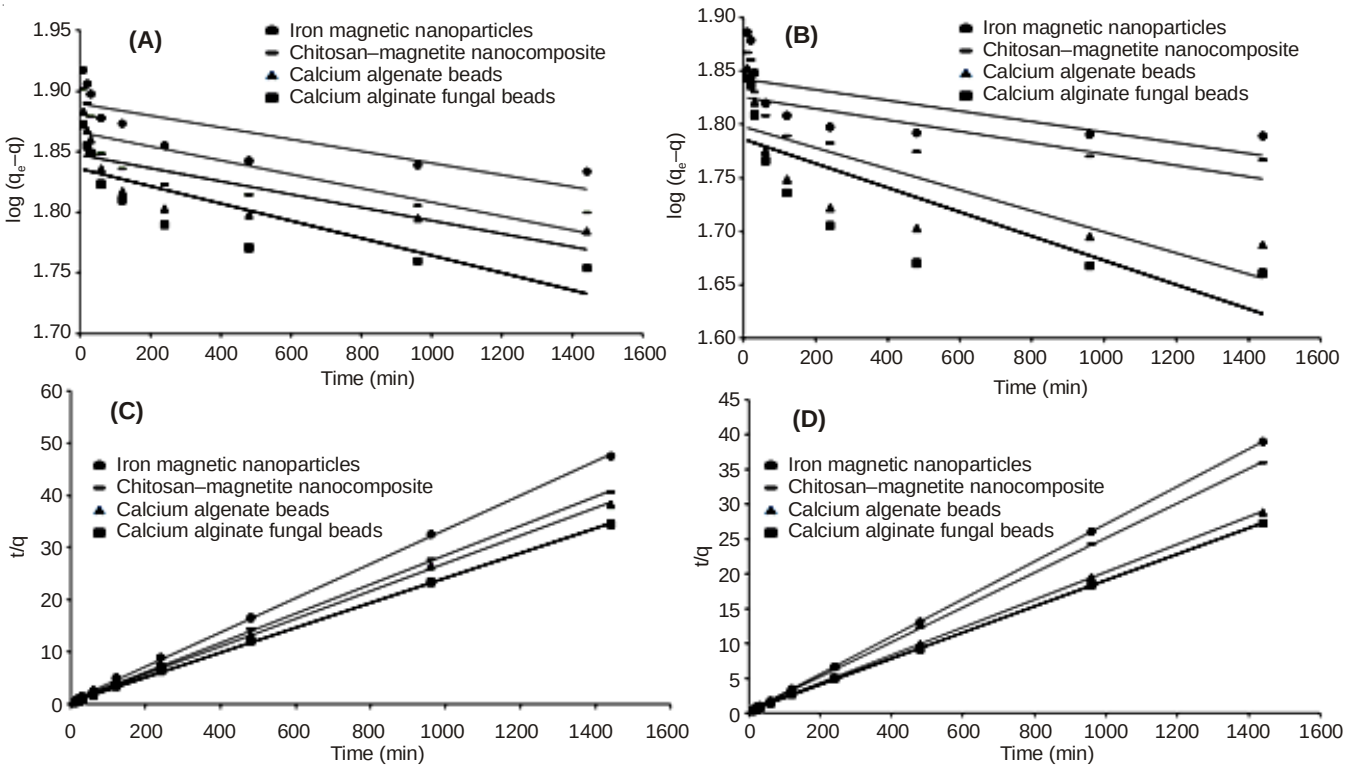

Fig. 6. Kinetic models: (A) and (B) pseudo first order for Ag(I) and Cr(VI), (C) and (D) pseudo second order for Ag(I) and Cr(VI) (explanations as given in Fig. 2)

beads. The results obtained suggest that pseudo second order model fitted well to the data because the q_t value and correlation coefficient (R^2) obtained in case of pseudo second order model was in close agreement with that of experimental value[46].

Conclusion

Four types of adsorbents (iron magnetic nanoparticles, chitosan–magnetite nanocomposite, calcium algenate beads and calcium alginate fungal beads) were studied for the adsorption of Ag(I), Cr(VI) and Pb(II) ions from simulated aqueous solutions. The adsorption efficiencies were found higher and comparable for calcium alginate fungal beads and chitosan–magnetite nanocomposite *versus* iron magnetic nanoparticles and calcium algenate beads. The maximum sorption capacities of chitosan–magnetite nanocomposite, calcium alginate fungal beads, calcium algenate beads and iron magnetic nanoparticles for Ag(I) were recorded to be 93.97, 93.48, 83.41 and 73.3 mg g^{-1}, whereas 95.21, 91.03, 75.43 and 68.75 mg g^{-1} were recorded for Cr(VI) at equilibrium time and Pb(II) adsorption was similar to Ag(I). Adsorption behaviours varied with respect to initial pH, initial metal ions concentration and contact time. The pseudo-second order kinetic model and Freundlich isotherm model fitted well to the adsorption data. The removal of Ag(I), Cr(VI) and Pb(II) ions by using adsorbent under investigation is suggested.

REFERENCES

1. R.S. Vieira and M.M. Beppu, *Water Res.*, **40**, 1726 (2006).
2. Q. Manzoor, R. Nadeem, M. Iqbal, R. Saeed and T.M. Ansari, *Bioresour. Technol.*, **132**, 446 (2013).
3. I. Ullah, R. Nadeem, M. Iqbal and Q. Manzoor, *Ecol. Eng.*, **60**, 99 (2013).
4. J. Hu, D. Zhao and X. Wang, *Water Sci. Technol.*, **63**, 918 (2011).
5. M. Iqbal, I.A. Bhatti, M. Zia-Ur-Rehman, H.N. Bhatti and M. Shahid, *Asian J. Chem.*, **26**, 4291 (2014).
6. N. Bilal, S. Ali and M. Iqbal, *Asian J. Chem.*, **26**, 1882 (2014).
7. D. Park, Y.-S. Yun and J.M. Park, *Chemosphere*, **60**, 1356 (2005).
8. A. Pethkar and K. Paknikar, *Process Biochem.*, **38**, 855 (2003).
9. Q. Manzoor, R. Nadeem, M. Iqbal, R. Saeed and T.M. Ansari, *Bioresour. Technol.*, **132**, 446 (2013).
10. J. Iqbal, F. Cecil, K. Ahmad, M. Iqbal, M. Mushtaq, M. Naeem and T. Bokhari, *Asian J. Chem.*, **25**, 2099 (2013).
11. I.A. Bhatti, M.A. Hayat and M. Iqbal, *J. Chem. Soc. Pak.*, **34**, 1012 (2012).
12. R. Perveen, Y. Jamil, M. Ashraf, Q. Ali, M. Iqbal and M.R. Ahmad, *Photochem. Photobiol.*, **87**, 1453 (2011).
13. Z. ul Haq, Y. Jamil, S. Irum, M.A. Randhawa, M. Iqbal and N. Amin, *Pol. J. Environ. Stud.*, **21**, 369 (2012).
14. A. Naz, Y. Jamil, M. Iqbal, M.R. Ahmad, M.I. Ashraf and R. Ahmad, *Indian J. Biochem. Biophys.*, **49**, 211 (2012).
15. Y. Jamil, R. Perveen, M. Ashraf, Q. Ali, M. Iqbal and M.R. Ahmad, *Laser Phys. Lett.*, **10**, 045606 (2013).
16. Y. Jamil and M.R. Ahmad, *Pak. J. Bot.*, **44**, 1851 (2012).
17. S. Madala, S.K. Nadavala, S. Vudagandla, V.M. Boddu and K. Abburi, *Arabian J. Chem.*, **25**, 214 (2013).
18. H.A. Shahzad, Y. Jamil, M. Iqbal, M. Musadiq and M.A. Naeem, *Asian J. Chem.*, **26**, 1887 (2014).
19. N.R. Bishnoi, R. Kumar and K. Bishnoi, *Indian J. Exp. Biol.*, **45**, 657 (2007).
20. M.-W. Wan, I.G. Petrisor, H.-T. Lai, D. Kim and T.F. Yen, *Carbohydr. Polym.*, **55**, 249 (2004).
21. K. Krishnapriya and M. Kandaswamy, *Carbohydr. Res.*, **345**, 2013 (2010).
22. M. Monier, D. Ayad and D. Abdel-Latif, *Colloids Surf. B*, **94**, 250 (2012).
23. C.M. Futalan, C.-C. Kan, M.L. Dalida, K.-J. Hsien, C. Pascua and M.-W. Wan, *Carbohydr. Polym.*, **83**, 528 (2011).
24. S.R. Popuri, Y. Vijaya, V.M. Boddu and K. Abburi, *Bioresour. Technol.*, **100**, 194 (2009).
25. I. Jha, L. Iyengar and A.P. Rao, *J. Environ. Eng.*, **114**, 962 (1988).
26. R. Laus and V.T. De Favere, *Bioresour. Technol.*, **102**, 8769 (2011).

27. M. Monier and D. Abdel-Latif, *J. Hazard. Mater.*, **209-210**, 240 (2012).
28. N. Gupta, A.K. Kushwaha and M. Chattopadhyaya, *J. Taiwan Inst. Chem. Eng.*, **43**, 604 (2012).
29. W. Ngah and S. Fatinathan, *J. Environ. Manage.*, **91**, 958 (2010).
30. M. Suguna, N. Siva Kumar, A. Subba Reddy, V. Boddu and A. Krishnaiah, *Can. J. Chem. Eng.*, **89**, 833 (2011).
31. P. Xiangliang, W. Jianlong and Z. Daoyong, *Process Biochem.*, **40**, 2799 (2005).
32. F. Gilleta, C. Roisin, M.A. Fliniaux, A. Jacquin-Dubreuil, J.N. Barbotin and J.E. Nava-Saucedo, *Enzyme Microb. Technol.*, **26**, 229 (2000).
33. T.H. Bokhari, M. Kashif, I.A. Bhatti, M. Zubair, S. Adeel, M. Yousaf, M. Ahmad, M. Iqbal, M. Usman, M. Zuber and A. Mansha, *Asian J. Chem.*, **25**, 8668 (2013).
34. F.A. Al-Rub, M. El-Naas, F. Benyahia and I. Ashour, *Process Biochem.*, **39**, 1767 (2004).
35. K. Tsekova, D. Todorova, V. Dencheva and S. Ganeva, *Bioresour. Technol.*, **101**, 1727 (2010).
36. S.-H. Huang and D.-H. Chen, *J. Hazard. Mater.*, **163**, 174 (2009).
37. M. Namdeo and S. Bajpai, *Colloids Surf. A*, **320**, 161 (2008).
38. C. Gok and S. Aytas, *J. Hazard. Mater.*, **168**, 369 (2009).
39. K. Akhtar, A. Khalid, M. Akhtar and M. Ghauri, *Bioresour. Technol.*, **100**, 4551 (2009).
40. H.N. Bhatti, B. Mumtaz, M.A. Hanif and R. Nadeem, *Process Biochem.*, **42**, 547 (2007).
41. Z. Aksu and E. Balibek, *J. Hazard. Mater.*, **145**, 210 (2007).
42. H. Bag, A.R. Türker, M. Lale and A. Tunçeli, *Talanta*, **51**, 895 (2000).
43. M. Vieira, R. Oisiovici, M. Gimenes and M.G.C. Silva, *Bioresour. Technol.*, **99**, 3094 (2008).
44. G. Bayramoglu, M. Yilmaz, A.Ü. Senel and M.Y. Arica, *Biochem. Eng. J.*, **40**, 262 (2008).
45. Y. Yao, F. Xu, M. Chen, Z. Xu and Z. Zhu, *Bioresour. Technol.*, **101**, 3040 (2010).
46. B. Preetha and T. Viruthagiri, *Sep. Purif. Technol.*, **57**, 126 (2007).